

Plastic Collapse Load of Continuous Composite Plate Girders

MASAHIRO KUBO and THEODORE V. GALAMBOS

Composite beams and girders with a reinforced concrete slab have different moment-curvature characteristics, depending on whether the moment is positive or negative. It is usually assumed^{1,4} for the maximum strength of the negative moment section that the concrete slab does not carry tensile stresses, but the reinforcing steel bars are considered to act compositely with the steel section. In the Load Factor Design (LFD) method of the *AASHTO Standard Specifications for Highway Bridges*,¹ the maximum strength of laterally braced I-shaped sections is determined based on the provision of compact or noncompact sections. A compact section is defined as a section that can reach the plastic moment and rotate inelastically at this constant plastic moment.

Recently (1986), the *AASHTO Guide Specification for Alternate Load Factor Design Procedures*² was published for the design of steel beam bridges using braced compact sections. This procedure was adopted as a logical extension of the existing LFD method and it is based on the Autostress Design (ASD) procedures.^{9,10,11} The resistance of continuous beam bridges is determined by the plastic-mechanism method. In this method, a considerable amount of plastic rotation is required at the negative moment sections of intermediate supports, and so the concept of an effective plastic moment⁵ was applied. The ultimate load was assumed to be reached when a composite section in positive bending reached the plastic moment. The usefulness of this method was confirmed by design examples and loading tests of an actual bridge.^{8,11,14}

Research^{17,18,19} on extending the ASD method to noncompact beams and plate girders is presently (1987) actively pursued. Schilling¹⁷ tested three plate girders to investigate the inelastic moment-rotation characteristics in negative bending and proposed a lower-bound curve for

plastic rotation. Vasseghi and Frank¹⁹ conducted 17 different loading tests by using three large-size, composite plate girders. Test results indicated composite girders can sustain higher positive moments than presently permitted by the AASHTO Specification.¹ Parametric studies on continuous girders were also performed by Schilling¹⁸ and this study demonstrated the ASD method provides weight savings compared with the LFD method for noncompact girders as well as for compact rolled beams.

The object of this study is to pursue the applicability of the Autostress Design method for continuous composite girders. The ultimate bending strength and the moment-rotation characteristics are investigated first using the experimental data of noncompact beams and plate girders and then an idealized moment-curvature curve for the negative moment section is proposed. Finally, a simple plastic analysis of two-span continuous composite girders is presented and discussed.

ULTIMATE BENDING STRENGTH OF PLATE GIRDERS

The ultimate bending strength of I-shaped beams and girders is affected by instabilities such as lateral-torsional buckling, flange local buckling and web buckling. In the *AISC Load and Resistance Factor Design (LRFD) Specification*,⁴ the section is classified as a beam or a plate girder based on the flexural strength criterion for web slenderness, $h_c/t_w = 970/\sqrt{F_{yf}}$, where h_c is twice the distance from the neutral axis to the compression flange. The beam design criterion provides the limit states of lateral-torsional buckling (LTB), flange local buckling (FLB) and web local buckling (WLB); and the nominal bending strength M_n is determined by the lowest value of these limit states. The M_n of a compact beam is equal to the full plastic moment M_p .

For plate girders, the critical flexural stress F_{cr} determined by the lateral-torsional or local buckling of the compression flange, is used in computing the M_n of a plate girder. The strength reduction due to elastic web buckling is expressed to be linearly proportional to the ratio of web

Masahiro Kubo is Associate Professor, Department of Civil Engineering, Meijo University, Tenpaku, Nagoya, Japan.

Theodore V. Galambos is Professor, Department of Civil and Mineral Engineering, University of Minnesota, Minneapolis, Minnesota.

Table 1. Comparison of Experimental and Nominal Strengths of Plate Girders

Ref. No.	Test Girder	Yield Stress		$\frac{b_f}{2t_f}$	$\frac{h_c}{t_w}$	$\frac{M_u}{M_p}$	AISC/LRFD Spec.		$\frac{M_{pe}}{M_p}$
		F_{yf} (ksi)	F_{yw} (ksi)				Limit State	$\frac{M_u}{M_n}$	
15	No. 1	55.12	64.65	14.29	176.2	0.687	PG	1.015	0.196
	No. 2	53.97	64.49	14.29	173.9	0.689	PG	1.011	0.199
	No. 3	54.42	57.74	14.29	154.2	0.708	PG	1.021	0.204
	No. 4	54.66	59.62	14.26	153.7	0.690	PG	1.000	0.203
	No. 5	54.33	61.83	14.14	110.6	0.726	FLB	0.980	0.226
	No. 6	55.32	59.52	14.18	109.3	0.723	FLB	0.972	0.225
	No. 10	61.56	57.64	11.46	149.2	0.807	PG	1.004	0.291
12	WS - 3	46.80	41.70	9.67	115.3	0.863	WLB	0.949	0.467
	WS - 4	46.80	41.70	9.67	137.8	0.879	WLB	1.094	0.422
13	WS-12-N	34.70	42.00	14.67	104.1	0.915	FLB	1.065	0.341
	WS-13-N	34.70	42.00	14.67	113.0	0.881	FLB	1.027	0.323
7	GA	39.30	46.11	6.86	117.8	0.992	WLB	1.100	0.734
	GE	39.30	46.11	6.81	117.7	0.962	WLB	1.068	0.689
17	US	59.40	65.20	9.03	137.9	0.677	PG	1.000	0.252
	UL	58.20	65.20	9.15	128.2	0.812	PG	1.024	0.367
	SL	49.60	65.20	9.88	171.4	0.889	PG	1.013	0.400

Note: FLB = flange local buckling; WLB = web local buckling; PG = calculated by the plate girder provisions; M_{pe} = effective plastic moment.

area to compression flange area A_w/A_f and to the web slenderness ratio h_c/t_w . For the case of $F_{cr} = F_{yf}$ and $h_c/t_w = 970/\sqrt{F_{yf}}$, M_n is equal to the yield moment M_y .

Test results^{7,12,13,15,17} of laterally braced beams and girders are summarized in Table 1. All the test specimens have $h_c/t_w > 100$ and do not satisfy the criteria of the compact section in the LRFD Specification.⁴ In the table, the ratio of experimental ultimate moment to the nominal bending strength calculated using the LRFD Specification M_u/M_n is given. Good predictions are obtained for both the noncompact beam and the plate girder sections (mean ratio = 1.02, coefficient of variation = 0.04). In case of the plate girders with large web slenderness, the same types of results⁶ were also obtained. Thus, the ultimate bending moment M_u of a plate girder will be quite closely predicted from the nominal bending strength equations M_n in the AISC LRFD Specification. In Table 1, the column M_{pe} indicates an effective plastic moment used in place of the actual plastic moment M_p in the Autostress design method.^{9,10,11}

MOMENT-CURVATURE RELATIONSHIP OF PLATE GIRDERS

Typical moment-rotation curves of laterally braced members are illustrated in Fig. 1. Compact sections are capable of reaching the plastic moment capacity M_p . Sections suitable for plastic design must be able to reach their plastic moment and, in addition, must achieve considerable inelastic rotation before the onset of local buckling. The ro-

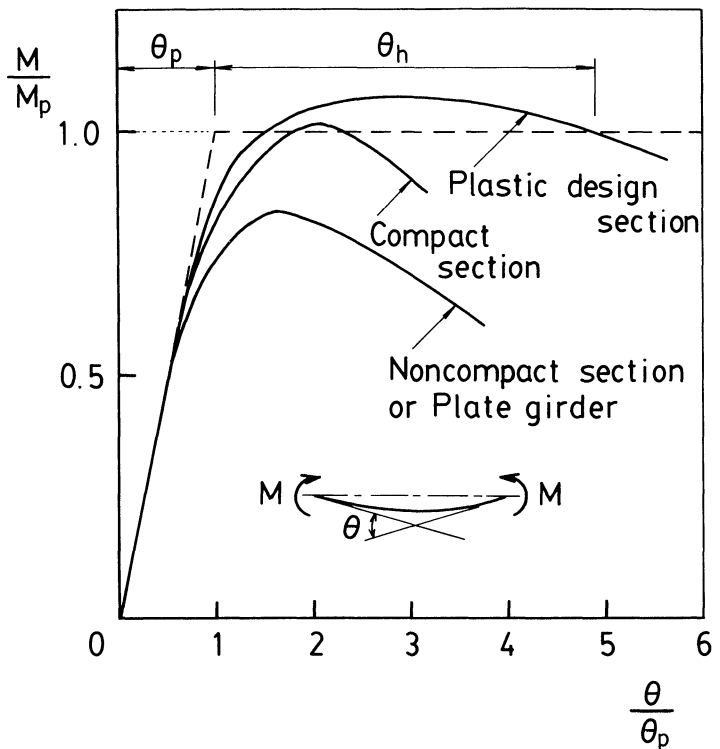


Figure 1. Typical moment-rotation characteristic curves

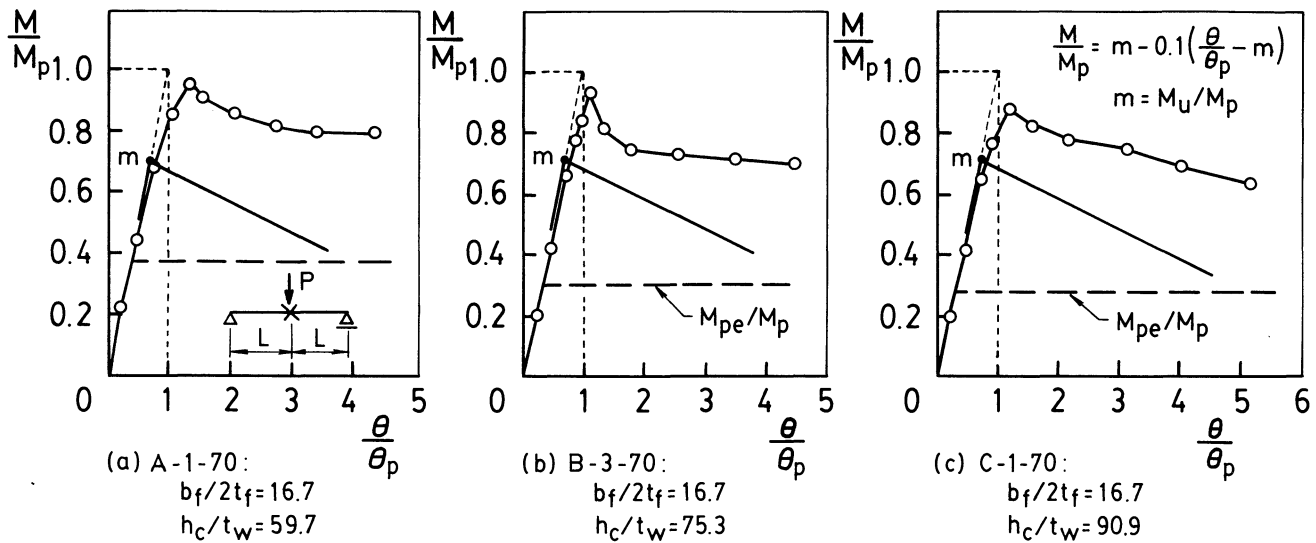


Figure 2. Moment-rotation curves of noncompact beams

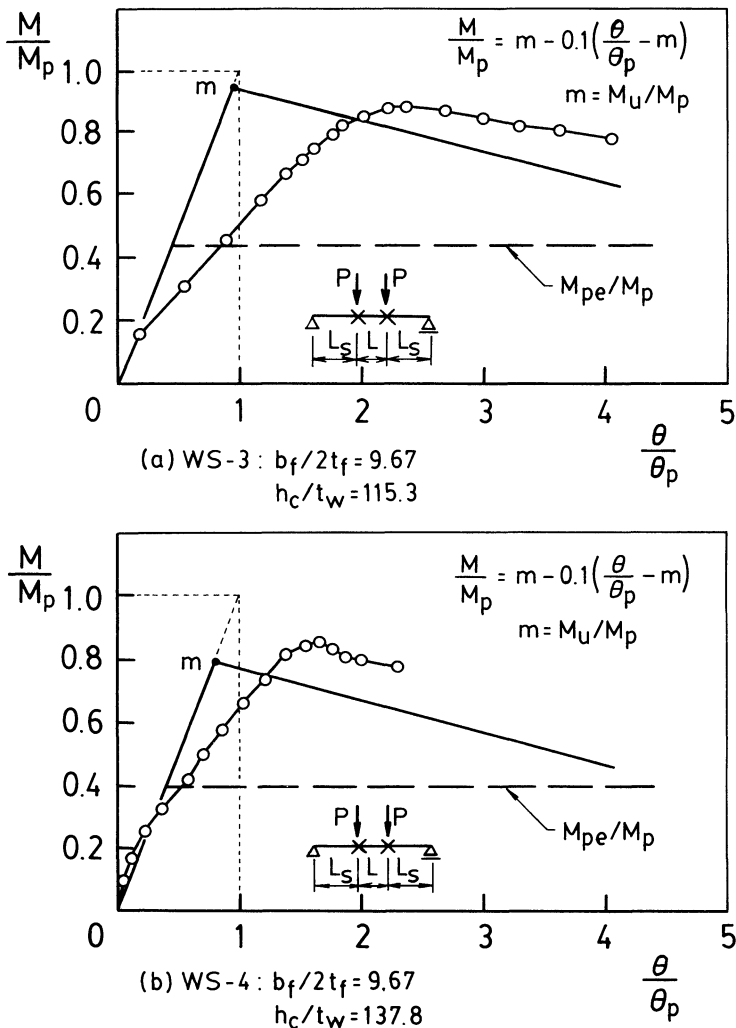


Figure 3. Moment-rotation curves of noncompact beams

tation capacity $R = \Theta_h/\Theta_p$, shown in the figure, is used commonly to measure this ductility. Θ_p and Θ_h are, respectively, the elastic and plastic components of the rotation prior to the moment falling below M_p . In noncompact sections having a relatively large width-thickness ratio of flange or web, premature failure due to local buckling will occur and the strength does not reach to M_p .

Test results¹⁶ of simply supported beams under a central concentrated load are shown in Figs. 2a, b and c. The beams are supported laterally at mid-span and at the end-supports. The width-thickness ratio $b_f/2t_f$ of the flange is a constant value of 16.7, while the width-thickness ratios h_c/t_w of the web vary as follows: 59.7, 75.3 and 90.9. All the test beams failed by local buckling of the compression flange. It can be seen the moment capacity reduces as the ratio of h_c/t_w increases, but there is no distinct difference in the moment-curvature curves. In the figures, the ultimate bending strength $m = M_u/M_p$ (limit state: FLB) calculated from the AISC LRFD Specification is given and the ratios of test-strength to prediction ranged from 1.23 to 1.36.

Test curves¹² of the moment-curvature relationship for noncompact beams which failed by web local buckling are shown in Figs. 3a and 3b. These beams were tested under uniform moment. The flange width-thickness $b_f/2t_f$ of 9.67 just meets the compactness limit of $b_f/2t_f = 65/\sqrt{F_{yf}}$. Although an early departure from elastic linearity is obtained in the moment-curvature relationship, the moment capacity is well predicted by the value of $m = M_u/M_p$ (limit state: WLB) of the LRFD Specification.⁴

Test results¹⁷ of three transversely stiffened girders without longitudinal stiffeners are presented in Figs. 4a, b and c. Specimen US and UL are unsymmetrical sections with a smaller compression flange than the tension flange. The flange and web slenderness ratios of three specimens were close to the limiting values in the AASHTO LFD cri-

teria¹ for braced, noncompact sections. The moment-rotation curves agreed well with the theoretical values in the elastic range. For all the specimens, $m = M_u/M_p$ was determined by the LRFD design provision for plate girders.

In this study, the moment-curvature behavior for noncompact beams and plate girders is assumed to be simply elastic-softening as follows:

$$\frac{M}{M_p} = \frac{\theta}{\theta_p} \text{ when } 0 < \frac{\theta}{\theta_p} < m \quad (1)$$

$$\frac{M}{M_p} = m + k \left(\frac{\theta}{\theta_p} - m \right) \text{ when } \frac{\theta}{\theta_p} > m \quad (2)$$

in which m is the ratio of ultimate bending moment to full plastic moment and $= M_u/M_p$; k is the slope of softening of the bending moment-curvature relationship.

Comparison between the experimental curve and the idealized relationship using $k = -0.1$ is shown in Figs. 2, 3 and 4. This idealization gives a very conservative estimate for beams under moment gradient, as shown in Fig. 2. However, it can be seen the correlation between the experimental and idealized curves becomes better as the web width-thickness ratio increases.

The following effective plastic moment is used in the AASHTO Guide Specification². The effective plastic moment M_{pe} is a reduced moment that accounts for the effects of local buckling and is expressed as

$$M_{pe} = R_f M_{pf} + R_w M_{pw} \quad (3)$$

where M_{pf} , M_{pw} are the flange and web components of the full plastic moment, respectively. The reduction factors, R_f and R_w are given by

$$R_f = 0.0845 \frac{E}{F_{yf}} \left(\frac{t_f}{b'} \right)^2 \leq 1 \quad (4)$$

$$R_w = 1.32 \frac{E}{F_{yf}} \left(\frac{t_w}{D_{cp}} \right)^2 \leq 1 \quad (5)$$

where

- b' = the width of the projecting compression flange
- E = Young's modulus
- D_{cp} = the distance to the compression flange from the neutral axis for plastic bending
- F_{yf} = yield stress of the flange plate.

Equations 4 and 5 are derived from the limiting width-thickness ratios of the flange and web for the plastic design section in Part 2 of the AISC Specification.³ In Figs. 2, 3 and 4, the level of M_{pe}/M_p is described by a dotted line. This idealization gives considerably lower values of the moment-curvature relationships for noncompact beams and girders.

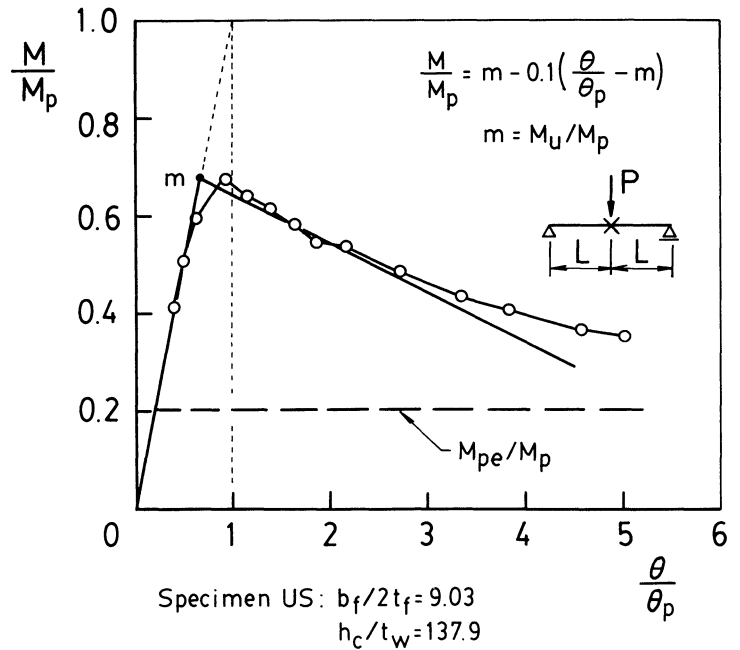


Figure 4a. Moment-rotation curve of of plate girder

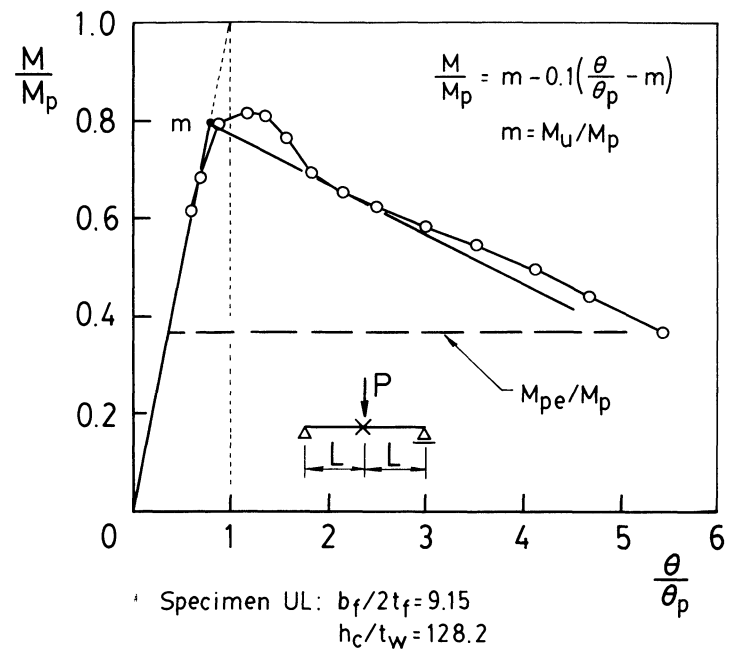


Figure 4b. Moment-rotation curve of of plate girder

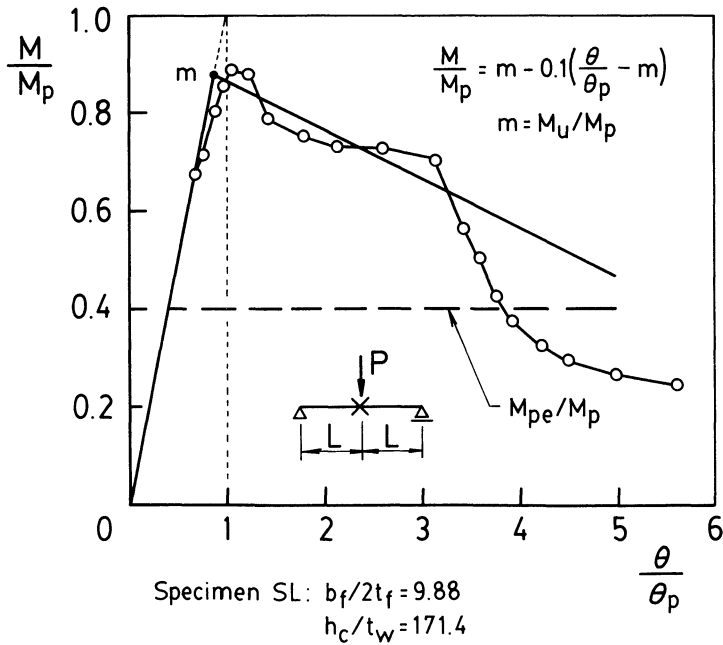


Figure 4c. Moment-rotation curve of of plate girder

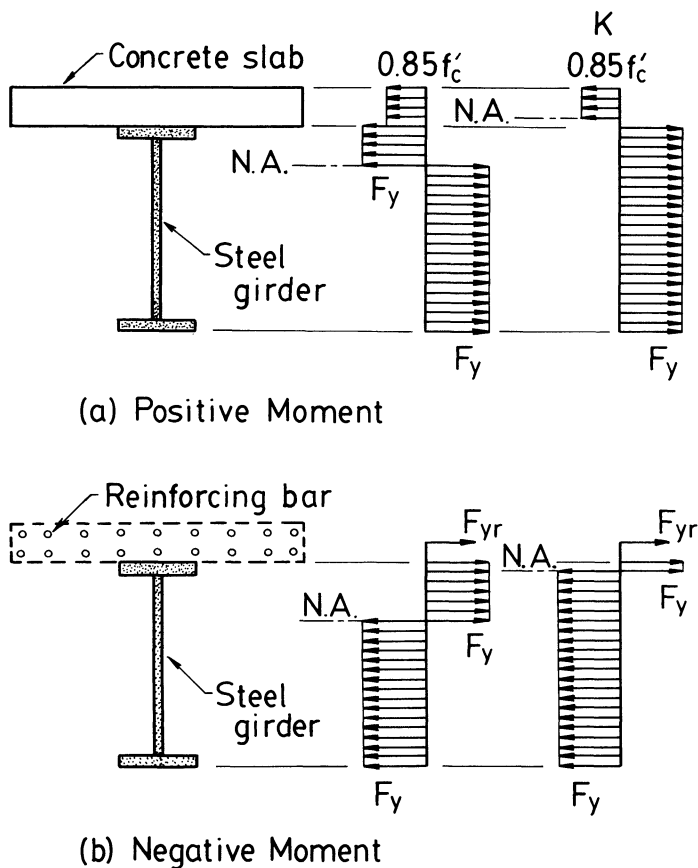


Figure 5. Plastic stress distribution for composite girders

BENDING STRENGTH AND MOMENT-CURVATURE RELATIONS OF COMPOSITE GIRDERS

The maximum strength of composite beams and girders with reinforced concrete slab differs depending on the positive and negative bending sections. For compact sections in positive bending, the maximum strength can be computed from the resultant moment of the fully plastic stress distribution acting on the composite section (see Fig. 5a). In case of negative bending, it is assumed the concrete slab does not carry tensile stresses. The maximum strength of the compact sections can be computed from the full plastic moment of the steel section including reinforcing steel bars (Fig. 5b). When a noncompact section is used the maximum strength is limited by the moment at first yielding in the AASHTO Specification.¹

In this study, the maximum strength of noncompact beams and plate girders in negative bending is evaluated by the procedures just described. Consider a composite girder section⁸ shown in Fig. 6 and assume all the cross-sectional dimensions except for the web depth h are constant. Assume the steel girder has a yield strength $F_y = 50$ ksi and the reinforcing steel bar has a yield strength $F_{yr} = 60$ ksi. The width-thickness ratio $b_f/2t_f$ of the flange equals the limiting value for compact section in the AISC LRFD Specification.⁴

The ultimate bending strength M_u/M_p of the negative moment section is shown in Fig. 7a. Two cases of the area of reinforcing steel ($A_r = 0, 6.16$ in.²) are given. The distance from the neutral axis to the inside face of the compression flange $h_c/2$ increases due to the reinforcing steel, and so ultimate strength decreases. The web limit of transversely stiffened girders in the AASHTO LFD method is $h_c/t_w = 163$ for $F_y = 50$ ksi steel. The ratios M_u/M_p corresponding to this limit are 0.843 for $A_r = 0$ and 0.791 for $A_r = 6.16$ in.², respectively. The idealized moment-curvature relationship of a negative bending section is shown in Fig. 7b. The elastic softening curve is given by using $m = 0.791$ and $k = -0.1$ in Eq. 2. The effective plastic moment M_{pe} according Eq. 3 was 46% of the negative plastic moment and this horizontal line intersects the softening line at $\Theta/\Theta_p = 4.1$.

SIMPLE PLASTIC ANALYSIS OF CONTINUOUS COMPOSITE GIRDERS

In this analysis, a two-span continuous girder (Fig. 8) is considered. The girder section consists of the composite section with a steel I-girder and a reinforced concrete slab (Fig. 6). Plastic moments of the composite girder in Fig. 5 are expressed by M_{pc} for the positive moment and M_{pn} for the negative moment, respectively and the following relation exists.

$$M_{pc} = \alpha M_{pn}, \alpha > 1 \quad (6)$$

The flexural rigidity is EI_c in the positive moment region and EI_n in the negative moment region. In the elas-

tic bending moment diagram the largest value occurs at the intermediate support 2 and therefore the bending moment M_2 reaches the ultimate moment, $M_u = m M_{pn}$, for negative bending. The non-dimensionalized load can be written:

$$\frac{PL}{M_{pc}} = 16 \left(\frac{\gamma_2}{\gamma_1} \right) \frac{m}{\alpha} \quad (7)$$

in which L is the span length and the coefficients γ_1 and γ_2 are

$$\gamma_1 = -1 + 12\beta^2 - 8\beta^3 + \frac{I_c}{I_n} (4 - 12\beta^2 + 8\beta^3) \quad (8)$$

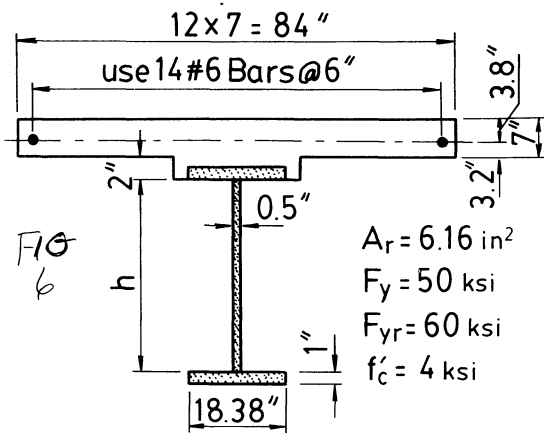


Figure 6. Cross-section of composite girder

$$\gamma_2 = \beta^3 + \frac{I_c}{I_n} (1 - \beta^3) \quad (9)$$

The parameter β defines the location of the point of zero moment and Eq. 10 must be satisfied

$$\beta = \frac{1}{\frac{\gamma_1}{8\gamma_2} + 1} \geq 0.727 \quad (10)$$

After the limiting value M_u is reached, the negative bending moment M_2 at the intermediate support changes in a

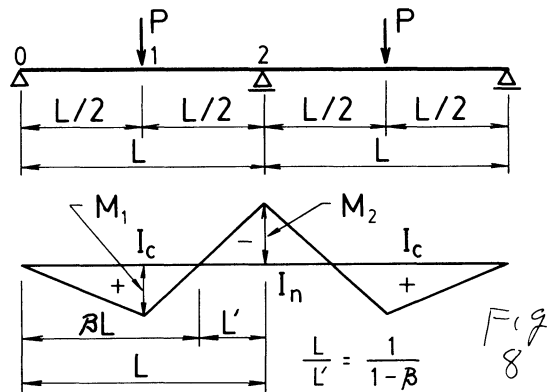


Figure 8. Continuous girder and bending moment

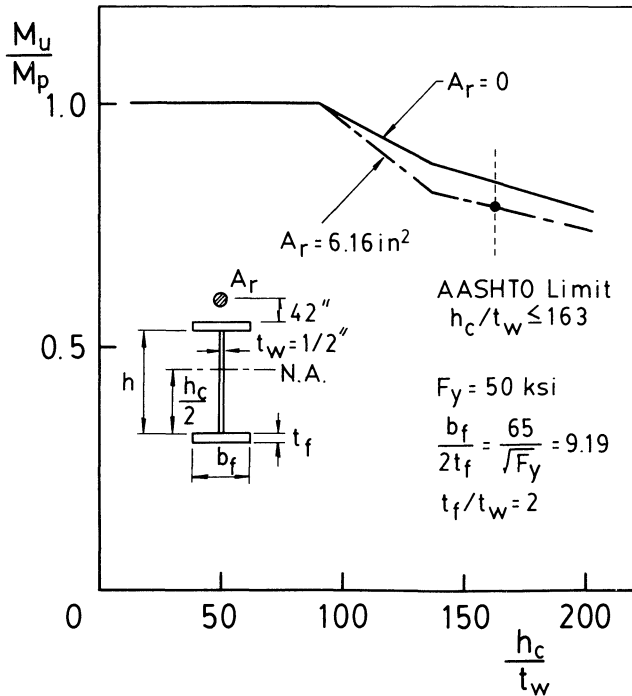


Figure 7a. Ultimate strength of negative moment section

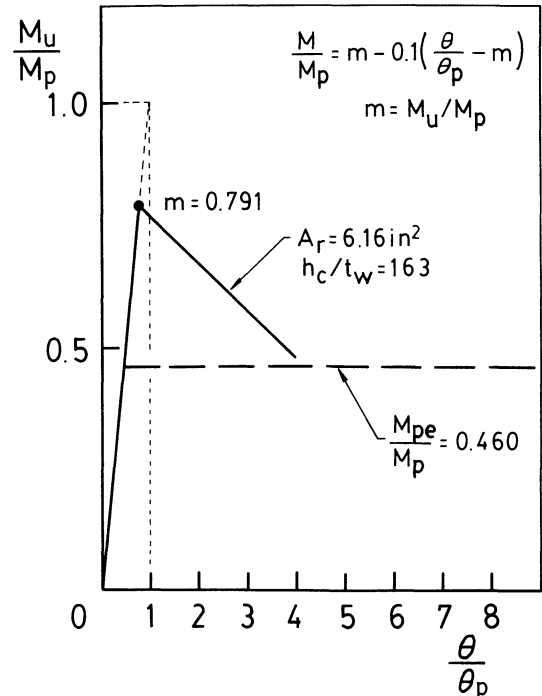


Figure 7b. Idealized moment-curvature relationships

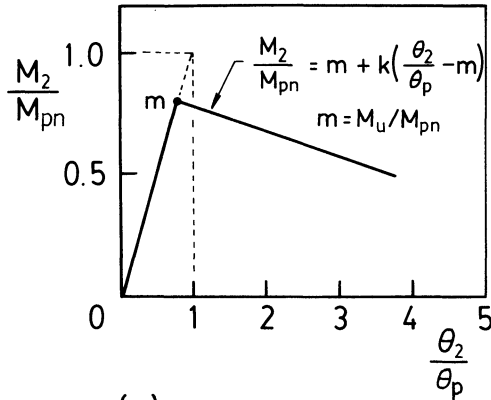
softening moment-curvature mode, shown in Fig. 9a as:

$$\frac{M_2}{M_{pn}} = m + k \left(\frac{\Theta_2}{\Theta_p} - m \right) \quad (11)$$

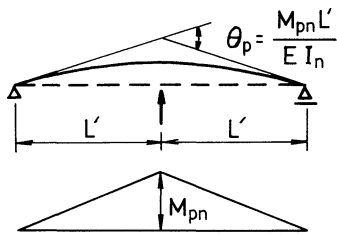
where Θ_p is defined as shown in Fig. 9b.

Furthermore, considering the correspondence with the negative moment regions in Fig. 8, Eq. 11 is modified as follows:

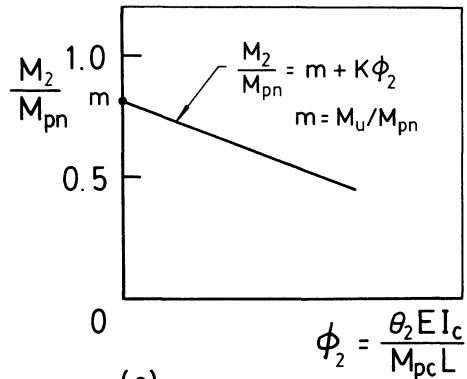
$$\frac{M_2}{M_{pc}} = \frac{1}{\alpha} (m + K\phi_2) \quad (12)$$



(a)



(b)



(c)

Figure 9. Moment-curvature relationships

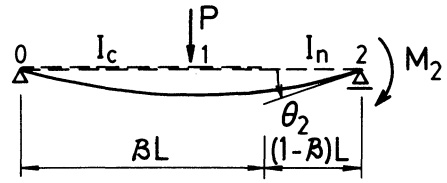


Figure 10. Deformation of girder

in which ϕ_2 is a rotation in the inelastic region (Fig. 9c) and is given by

$$\phi_2 = \frac{\Theta_2 EI_c}{M_{pc} L} \quad (13)$$

The slope of softening curvature is expressed by Eq. 14:

$$K = k \frac{\alpha}{(1-\beta)} \frac{I_n}{I_c} \quad (14)$$

Next, for a simply supported girder, as in Fig. 10, the following equilibrium and compatibility conditions must be satisfied:

$$\frac{M_1}{M_{pc}} = \frac{PL}{4M_{pc}} - \frac{M_2}{2M_{pc}} \quad (15)$$

where M_1 is the maximum bending moment in the positive bending regions and

$$\frac{\Theta_2 EI_c}{M_{pc} L} = \phi_2 = \frac{\gamma_1 PL}{48M_{pc}} - \frac{\gamma_2 M_2}{3M_{pc}} \quad (16)$$

Substituting Eq. 12 into Eq. 16, Eq. 17 is obtained.

$$\frac{PL}{M_{pc}} = \frac{48}{\gamma_1} \left[\frac{\gamma_2 m}{3\alpha} + \left(1 + \frac{\gamma_2 K}{3\alpha} \right) \phi_2 \right] \quad (17)$$

The maximum positive bending moment M_1 can be expressed as:

$$\frac{M_1}{M_{pc}} = \frac{(8\gamma_2 - \gamma_1)m}{2\gamma_1\alpha} + \left[\frac{12}{\gamma_1} \left(1 + \frac{\gamma_2 K}{3\alpha} \right) - \frac{K}{2\alpha} \right] \phi_2 \quad (18)$$

In this analysis, it is also assumed that if the first hinge forms in positive bending, the limit state is reached. Putting $M_1 = M_{pc}$ into Eq. 18, the limiting value of rotation $\bar{\phi}_2$ at the intermediate support is

$$\bar{\Phi}_2 = \frac{1 - \frac{(8\gamma_2 - \gamma_1)m}{2\gamma_1\alpha}}{\frac{12}{\gamma_1} \left(1 + \frac{\gamma_2 K}{3\alpha}\right) - \frac{K}{2\alpha}} \quad (19)$$

Finally, the collapse load P_u of the continuous girder in Fig. 8 is

$$\frac{P_u L}{M_{pc}} = \frac{48}{\gamma_1} \left[\frac{\gamma_2 m}{3\alpha} + \frac{\left(1 + \frac{\gamma_2 K}{3\alpha}\right)}{\left\{ \frac{12}{\gamma_1} \left(1 + \frac{\gamma_2 K}{3\alpha}\right) - \frac{K}{2\alpha} \right\}} \times \left\{ 1 - \frac{(8\gamma_2 - \gamma_1)m}{2\gamma_1\alpha} \right\} \right] \quad (20)$$

Similarly, in case of a uniformly distributed load, the collapse load q_u is

$$\frac{q_u L^2}{M_{pc}} = \frac{24}{\gamma_1} \left[\frac{\gamma_2 m}{3\alpha} + \frac{\left(1 + \frac{\gamma_2 K}{3\alpha}\right)}{\left\{ \frac{3\beta(2-\beta)}{\gamma_1} \left(1 + \frac{\gamma_2 K}{3\alpha}\right) - \frac{\beta K}{2\alpha} \right\}} \times \left\{ 1 - \frac{\beta(4\gamma_2 - 2\beta\gamma_2 - \gamma_1)m}{2\gamma_1\alpha} \right\} \right] \quad (21)$$

In Eq. 21 the following coefficient, γ_i is used instead of Eq. 8,

$$\gamma_1 = 4\beta^3 - 3\beta^4 + \frac{I_c}{I_n} (1 - 4\beta^3 + 3\beta^4) \quad (22)$$

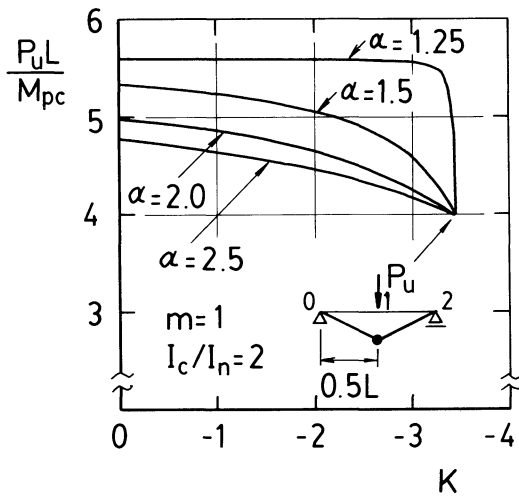


Figure 11. Collapse loads of continuous girder with concentrated loads

and the parameter β is defined by

$$\beta = 1 - \frac{\gamma_1}{4\gamma_2} \geq 0.75 \quad (23)$$

If we assume $\alpha = m = I_c/I_n = 1$ and $K = 0$ in Eqs. 20 and 21, the collapse loads of $P_u L/M_{pc} = 6$ and $q_u L^2/M_{pc} = 11.732$ are obtained, corresponding with the results of simple plastic theory.

NUMERICAL EXAMPLES AND DISCUSSION

Figures 11 and 12 show the non-dimensional collapse load $P_u L/M_{pc}$ in terms of various α and K values, taking $m = 1$ and 0.8 , for two-span continuous girders ($I_c/I_n = 2$; $\beta = 0.777$) under a central concentrated load at each span. Similarly, Figs. 13 and 14 show the results ($I_c/I_n = 2$; $\beta = 0.802$) for a uniformly distributed load. Minimum collapse loads are $P_u L/M_{pc} = 4$ for concentrated loads and $q_u L^2/M_{pc} = 8.326$ for a distributed load and are obtained at $K = -12m/\gamma_1$ and $-3\beta(2-\beta)m/\gamma_1$, respectively.

It can be seen the collapse load is affected considerably by the parameters α and m . The reduction of the collapse load due to the softening curvature (the parameter K) for the uniformly distributed load is larger than that of the concentrated load. The collapse loads for $\alpha = 1.25$ and 1.5 are compared with the value of simple plastic theory ($\alpha = m = I_c/I_n = 1$, $K = 0$) in Table 2. For the values of $\alpha = 1.5$, $m = 0.8$ and $K = -1$, the decrease in the collapse load is about 20%.

Next, numerical examples for a composite plate girder (web depth $h = 74.96$ in), shown in Fig. 6, are presented. The width-thickness ratios of a steel girder (yield strength $F_y = 50$ ksi) are 9.19 for the flange and 163 for the web, respectively, and both ratios are close to the AASHTO

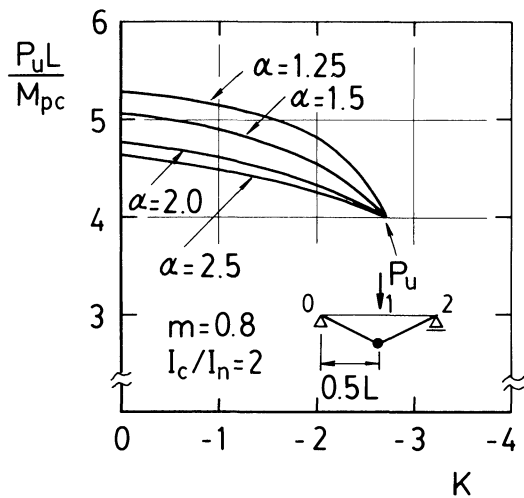


Figure 12. Collapse loads of continuous girder with concentrated loads

slenderness limits¹ for transversely stiffened girders. The plastic moments and flexural rigidities for the section are:

plastic moment for positive moment:

$$M_{pc} = 12,741 \text{ kip-ft,}$$

plastic moment for negative moment:

$$M_{pn} = 9,944 \text{ kip-ft}$$

flexural rigidity for positive moment:

$$EI_c = 27,953,986 \text{ kip-ft}^2,$$

and flexural rigidity for negative moment:

$$EI_n = 16,300,394 \text{ kip-ft}^2,$$

in which Young's modulus of steel $E = 29,000$ ksi and the ratio of E to Young's modulus of concrete $n = 8$ were used. The effective plastic moment for negative moment computed from Eq. 3: $M_{pe} = 4,582$ kip-ft ($R_f = 0.613$, $R_w = 0.115$).

The ultimate moment of a steel girder under negative moment, $M_u = 7,865$ kip-ft ($R_{pg} = 0.973$) was obtained from the LRFD Specification.⁴ The moment-curvature relationships for the negative moment, as in Fig. 7b, were used and the slope of softening was expressed by using $k = -0.1$. Therefore, the parameters for the application of Eqs. 20 and 21 can be determined as

$$\alpha = \frac{M_{pc}}{M_{pn}} = \frac{12,741}{9,944} = 1.281$$

$$m = \frac{M_u}{M_{pn}} = \frac{7,865}{9,944} = 0.791$$

$I_c/I_n = 1.715$; $\beta = 0.766$ for concentrated loads and $\beta = 0.791$ for uniformly distributed load.

$$K = k \frac{\alpha}{(1 - \beta)} \frac{I_n}{I_c}$$

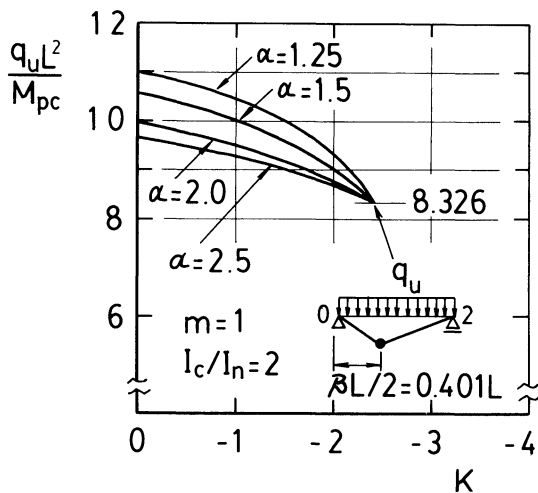


Figure 13. Collapse loads of continuous girder with uniformly distributed load

Table 2a. $P_u L / (6M_{pc})$. Values for Concentrated Load

K	$\alpha = 1.25$		$\alpha = 1.5$	
	$m = 1$	$m = 0.8$	$m = 1$	$m = 0.8$
0	0.933	0.880	0.888	0.844
-1	0.932	0.857	0.874	0.816

Table 2b. $q_u L^2 / (11.732 M_{pc})$. Values for Uniformly Distributed Load

K	$\alpha = 1.25$		$\alpha = 1.5$	
	$m = 1$	$m = 0.8$	$m = 1$	$m = 0.8$
0	0.937	0.892	0.899	0.861
-1	0.893	0.831	0.865	0.805

For concentrated loads

$$K = -0.1 \times \frac{1.281}{(1 - 0.766)} \times \frac{1}{1.715} = -0.319$$

and for the uniformly distributed load

$$K = -0.1 \times \frac{1.281}{(1 - 0.791)} \times \frac{1}{1.715} = -0.357$$

The values of the collapse load using four different moment-curvature relationships are listed in Table 3. Case 1 indicates the collapse load taking account of web buckling at the intermediate support. The collapse loads decrease 7% from the analysis which neglected such an ef-

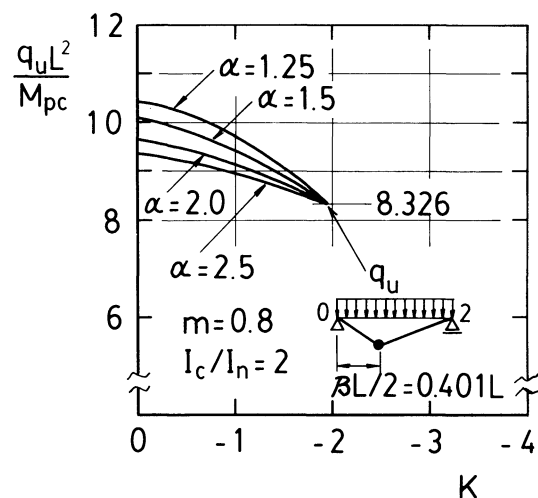
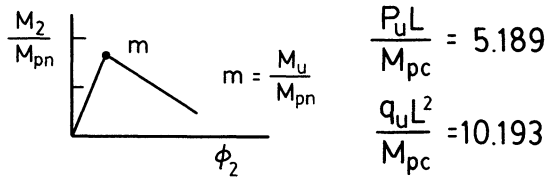


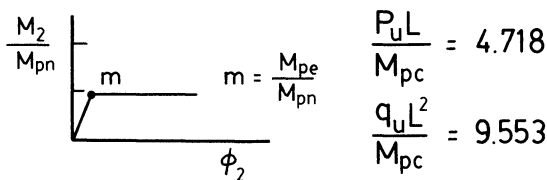
Figure 14. Collapse loads of continuous girder with uniformly distributed load

Table 3. Collapse Loads of Composite Plate Girder

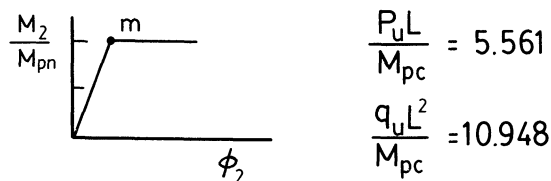
Case 1 : $\alpha = 1.281, m = 0.791, K = -0.319(-0.357)$ *



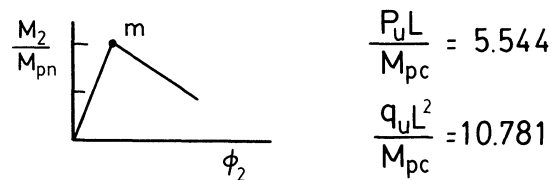
Case 2 : $\alpha = 1.281, m = 0.460, K = 0$



Case 3 : $\alpha = 1.281, m = 1, K = 0$



Case 4 : $\alpha = 1.281, m = 1, K = -0.319(-0.357)$ *



fect (Case 3). On the other hand, the collapse loads in Case 2 decrease 14% from those of Case 3. Thus the concept of using the effective plastic moment M_{pe} may give a conservative estimation for the composite plate girders. It can be seen from the comparison of Case 3 and Case 4 that the effect of softening in the moment-curvature relations on the collapse load is relatively small.

CONCLUSIONS

Basic problems in the application of Autostress design procedures to noncompact beams and plate girders are considered in this paper. The ultimate bending strength and the moment-rotation capacity were investigated based on the experimental results of girders with relatively slender webs. An elastic-softening curve was proposed as a

* Used for uniformly distributed load

moment-curvature relationship for the negative moment section of composite girders. The ultimate bending strength of steel girders can be determined by using the design procedure in the AISC LRFD Specification.

As numerical examples, two-span continuous girders were analyzed. The collapse load is affected largely by the ratio of the resistant moments in the positive and negative moment sections. For actual composite plate girders the effect of the softening on the collapse load is relatively small so that the parameter K of Eq. 14 may be expressed with the value of -0.5 . In the case of plate girders, the concept of using the effective plastic moment gives a conservative result for the collapse load.

Although the interaction with shear strength was neglected in this study, the Autostress Design procedures also could be applied to the transversely stiffened plate girders specified in the AASHTO Specification by means of a suitable moment-rotation curve for the negative moment section.

REFERENCES

1. American Association of State Highway and Transportation Officials *Standard Specifications for Highway Bridges* 13th Ed., Washington, D.C., 1983.
2. American Association of State Highway and Transportation Officials *Guide Specification for Alternate Load-Factor Design Procedures for Steel Beam Bridges Using Braced Compact Sections* 1986, Washington, DC.
3. American Institute of Steel Construction *Specification for the Design, Fabrication and Erection of Structural Steel for Buildings*, 8th Ed., Chicago, Ill., 1980.
4. American Institute of Steel Construction *Load and Resistance Factor Design Specification for Structural Steel Buildings* 1st Ed., Chicago, Ill., 1986.
5. Carskaddan, P.S., G. Haaijer and M.A. Grubb Computing the Effective Plastic Moment, *AISC Engineering Journal* 1st Qtr., 1982, pp. 12-15.
6. Cooper, P.B., T.V. Galambos and M.K. Ravindra LRFD Criteria for Plate Girders, *Journal of the Structural Division, ASCE* Vol. 104, No. ST9, September 1978, pp. 1389-1407.
7. Fukumoto, Y., K. Maegawa, Y. Itoh and Y. Asari Lateral-torsional Buckling Tests on Welded I-Girders under Moment Gradient *Proceedings of the Japan Society of Civil Engineers*, No. 362/I-4, October 1985, pp. 323-332 (in Japanese).
8. Grubb, M.A. Design Example Two-span Continuous Beam Highway Bridge Designed by the Autostress Method *Report on Project 188, AISI*, Washington, D.C., May 10, 1985.
9. Grubb, M.A. The AASHTO Guide Specification for Alternate Load-factor Design Procedures for Steel Beam Bridges *AISC Engineering Journal*, 1st Qtr. 1987, pp. 1-10.

10. *Haaijer, G., P.S. Carskaddan and M.A. Grubb* Autostress Design of Steel Bridges, *Journal of Structural Engineering*, Vol. 109, No. 1, January 1983, pp. 188–199.
11. *Haaijer, G., P.S. Carskaddan and M.A. Grubb* Suggested Autostress Procedures for Load Factor Design of Steel Beam Bridges *AISI Bulletin* No. 29, AISI, Washington, D.C., April 1987.
12. *Holtz, N.M. and G.L. Kulak* Web Slenderness Limits for Compact Beams *Structural Engineering Report No. 43*, University of Alberta, Alberta, Canada, March 1973.
13. *Holtz, N.M. and G.L. Kulak* Web Slenderness Limits for Compact Beams *Structural Engineering Report No. 51*, University of Alberta, Alberta, Canada, March 1975.
14. *Hourigan, E.V. and R.C. Holt* Design of a Rolled Beam Bridge by New AASHTO Guide Specification for Compact Braced Sections, *AISC Engineering Journal*, 1st Qtr., 1987, pp. 29–41.
15. *Johnson, D.L.* Buckling of Beam Compression Flanges *A Report Submitted to AISI*, Butler Manufacturing Company, November 1976.
16. *Ohtake, A. and F. Iwamuro* Load-Deformation Characteristic of Light-Gage I-Shaped Members, Part 1: Tests of Beams and Beam-Columns *Research Report No. 6104*, Research Institute of Sumitomo Metal Industry Corporation, Japan, March, 1982 (in Japanese).
17. *Schilling, C.G.* Moment-Rotation Tests of Steel Bridge Girders *Report on Project 188, AISI*, Washington, D.C., April 15, 1985.
18. *Schilling, C.G.* Exploratory Autostress Girder Designs *Report on Project 188, AISI*, Washington, D.C., July 1986.
19. *Vasseghi, A. and K.H. Frank* Static Shear and Bending Strength of Composite Girders *Final Report-Phase I, AISI Project 320A, Phil M. Ferguson Structural Engineering Laboratory Report* University of Texas, Austin, August 1986.